An Introduction to Lattice-Boltzmann

Georg Rempfer[1, a)]
Institute for Computational Physics (ICP), University of Stuttgart, Allmandring 3, 70569 Stuttgart, Germany

(Dated: October 11, 2016)

I. WHY LATTICE-BOLTZMANN

Traditional Langevin dynamics based MD simulations neglect hydrodynamic interaction and instead use a combination of random forces and friction (a constant particle mobility) as a model for fluid-particle interactions. In reality the mobility of and the forces acting on a particle in solution are determined by the momentum transport in the fluid and therefore depends on the presence and relative motion of other obects, such as solid walld or other particles. Langevin dynamics neglect the momentum transport in the fluid and therefore fail to correctly reproduce effects such as the reduces mobility of particles at solid interfaces, the concentration dependent conductivity of electrolytes, or the electrophoretic mobility of charged particles.

The effect the fluid exerts on the particles might not be the only reason to include a fluid model in an MD simulation, though. The coupling between fluid and particles allows for particles to drive fluid flow, such as in the case of electro-osmotic flow (EOF). Often this flow in itself is of interest, since it can serve as a tool in lab-on-a-chip devices and many other applications.

A natural way to include hydrodynamics in an MD simulations is to explicitly represent the fluid particles. This approach works but is limited to the smalles of systems, since fluid particles (such as H_2O) are typically small and light, and therefore limit the reachable length and time scales of the simulations when represented explicitly. Fortunately, a lot of the information contained in the fluid particles' trajectories isn't needed to model the previously mentioned effects, and any model correctly reproducing the momentum transport in the fluid suffices.

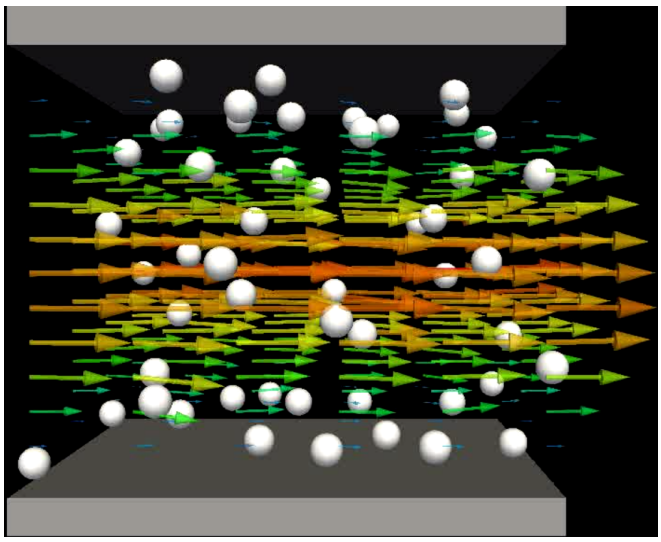

Figure 1. Snapshot of Poiseuille flow driven by sedimenting particles.

With lattice-Boltzmann, we pursue the approach of coupling the particles to a fluid dynamics solver. Several other methods, such as multi-particle collision dynamics (MPCD / SRD), dissipative particle dynamics (DPD), or smooth particle hydrodynamics (SPH) could serve for this purpose. The reason for not using more traditional CFD methods is that there performance stems in large parts from implicit time-stepping schemes, which allow one to use large, adaptively chosen time steps. They are typically unable to produce the 100s or even 1000s of solutions per second required to make MD simulations with their very small, explicit time steps of fixed size viable.

Fluid dynamics deals with the transport of mass, momentum, and in some cases energy, all of which are conserved quantities. To gain some understanding for the governing equations, let's first discuss conservation laws in physics and their mathematical description.

Note that hydrodynamic interactions only change dynamic observables (such as the rate at which a molecule passes a barrier) but not equilibrium quantities (such as the ratio of time, the molecule spends on one side of the barrier vs. the other).

II. CONSERVATION LAWS IN PHYSICS

All conservation laws in physics must be local conservation laws. This is a result of special relativity. Remember the ladder paradox shown in Fig. 2. The paradox deals with a ladder, which is too long to fit inside the garage when at rest. Due to length contraction, there is some speed at which the ladder fits in the garage as seen from the rest frame of the garage. Fig. 2a depicts this situation: the ladder moves through the garage at a speed, such that it exactly fits the garage. There is one point in time, when the doors at both ends of the garage close and the ladder is completely contained in the garage.

Fig. 2b depicts the same process as seem from the rest frame of the ladder. In this reference frame, the garage moves and appears contracted. When the garage moves over the ladder, there is no point at which the ladder is

[a)] Electronic mail: georg.rempfer@icp.uni-stuttgart.de

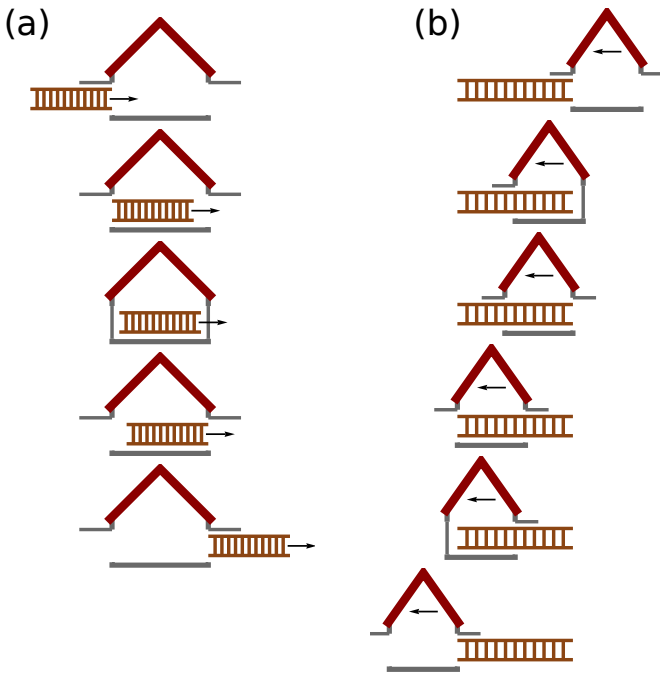

Figure 2. Ladder paradox.

completely contained in the garage and the two doors are never closed at the same time.

These seemingly contradictory observations are not a true paradox. This result is an actual prediction of special relativity and has been verified experimentally. The trick is that whether two spacially separated events (the closing of the one and the other door) happen simultaneously depend on the observer.

For exactly this reason, all conservation laws in physics must be local conservation laws. It is impossible that something, whose overall amount is conserved, disappears at one place and simultaneously appears at another. If this were the case, there would always be reference frames where it appears at the one place before it has disappeared at the other, or disappears at the one place and only later appears at the other.

For the mathematical description of a conservation law, this means that there is always a flux associated with a conserved quantity, and that this flux fulfills a continuity equation of the shape

$$\nabla \cdot \boldsymbol{j} = -\partial_t \rho. \tag{1}$$

Here ρ denotes the mass density and $\boldsymbol{j}$ the associated mass flux.

This continuity equation holds independently of the prescribed shape of the flux. The specifics of the system to be modeled enter exactly through the specific form of the flux.

III. CONSERVATION OF MOMENTUM

Since momentum is a conserved quantity as well, there has to be flux associated with the momentum density and there has to be a relation between the two with the shape similar to the continuity equation (1). We denote the momentum flux by $\bar{\boldsymbol{\Pi}}$ and the momentum density is given by $\rho\boldsymbol{u}$, with the mass density ρ, and the local velocity $\boldsymbol{u}$. The continuity equation then reads

$$\nabla \cdot \bar{\boldsymbol{\Pi}} = -\partial_t(\rho \boldsymbol{u}) + \boldsymbol{f}. \tag{2}$$

$\bar{\boldsymbol{\Pi}}$ is called the stress and the situation is complicated only by the fact that momentum is a vectorial quantity, which makes the stress a tensor. Imagine the stress tensor like this: the stress tensor is a 3×3 matrix at every point in space, which when multiplied by a normalized direction vector, yields the amount of momentum being transferred in that direction. This momentum of course is a vector. The external force $\boldsymbol{f}$ acts as an external source of momentum, which has to be accounted for.

So far, we have not specified any properties of our system and as a result, the equations for the transport of mass (1) and momentum (2) hold for all kinds of continuum media (solids, fluids, etc.). We obtain the governing equations for our fluid by speficying the expressions for the mass flux $\boldsymbol{j}$ and momentum flux $\bar{\boldsymbol{\Pi}}$:

$$\boldsymbol{j} = \rho \boldsymbol{u}, \tag{3}$$

$$\bar{\boldsymbol{\Pi}} = p\bar{\mathbb{1}} - \underbrace{\eta\left(\boldsymbol{\nabla u} + \boldsymbol{\nabla u}^T\right)}_{\text{viscous}} + \underbrace{\rho\, \boldsymbol{u} \otimes \boldsymbol{u}}_{\text{convective}}. \tag{4}$$

Viscous momentum transport happens in the direction of the shearing — sheets of faster moving fluid exert a force on slower moving sheets through friction. The shape of the convective momentum flux will become clear in Sec. VI. Combining Eqs. (1) – (4) with the requirement for incompressibility $\rho = \text{const.}$ results in the incompressible Navier-Stokes equations

$$\begin{aligned} \rho\left(\partial_t \boldsymbol{u} + (\boldsymbol{u} \cdot \boldsymbol{\nabla})\boldsymbol{u}\right) &= -\nabla p + \eta \boldsymbol{\nabla^2 u} + \boldsymbol{f}, \\ \nabla \cdot \boldsymbol{u} &= 0. \end{aligned} \tag{5}$$

IV. THE BOLTZMANN TRANSPORT EQUATION

Lattice-Boltzmann does not directly discretize the Navier-Stokes equations (5), instead it approximates the Boltzmann transport equation. Our aim for this section is to introduce the Boltzmann transport equation and to illustrate how to derive its equivalence to the Navier-Stokes equations.

The Boltzmann transport equation gives the time evolution of the single particle phase space distribution. For non-interacting particles (an ideal gas), it reads

$$\frac{d}{dt} f\big(\boldsymbol{x}(t), \boldsymbol{v}(t), t\big) = \partial_t f + \boldsymbol{v} \cdot \nabla_{\boldsymbol{x}} f + \frac{\boldsymbol{F}}{m} \cdot \nabla_{\boldsymbol{v}} f = 0, \tag{6}$$

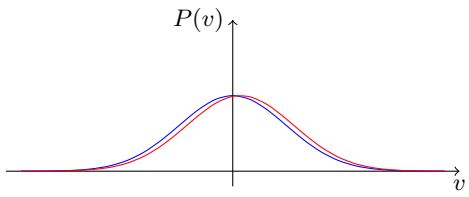

Figure 3. Velocity distribution of molecules at two different position in a typical subsonic flow. Blue: Fluid at rest (close to a no-slip boundary). Red: Fluid at a position of finite velocity.

where we have used the chain rule for the first equality. Remember that in phase space, trajectories don't cross, therefore you always find the same particles on a trajectory. The Boltzmann equation for an ideal gas says exactly that — that the density along a phase space trajectory stays constant.

In the case of scattering due to collisions of the particles amongst each other, we introduce the collision operator $\mathcal{C}[f]$, which provides the change of the phase space distribution due to interactions of the particles. Using the collision operator, the Boltzmann transport equation states

$$\partial_t f + \boldsymbol{v} \cdot \nabla_{\boldsymbol{x}} f + \frac{\boldsymbol{F}}{m} \cdot \nabla_{\boldsymbol{v}} f = \mathcal{C}[f]. \tag{7}$$

At first glimpse this equation seems simpler than the Navier-Stokes equations (5) due to its linearity. The whole complexity of the problem is hidden in the collision operator $\mathcal{C}$, which provides the change of an arbitrary phase space distribution die to interactions of the constituent particles. This object is exceedingly complex and there is no chance, that we could model it realistically. Luckily, that is not necessary, as any collsion operator which conserves mass and momentum and acts locally (particles interact through short ranged interactions) will reproduce the Navier-Stokes equations.

The simplest choice for a mass and momentum conserving collision operator is given by the so-called single relaxation time (SRT) collision operator

$$\mathcal{C}[f(\boldsymbol{x},\boldsymbol{v},t)] = \frac{1}{\tau}\Big(f^{\mathrm{eq}}\big(\rho(\boldsymbol{x}),\boldsymbol{u}(\boldsymbol{x})\big) - f(\boldsymbol{x},\boldsymbol{v},t)\Big). \tag{8}$$

with f^{eq} the velocity distribution in thermal equilibrium, a Boltzmann distribution in the kinetic energy (with the same mass and velocity as the local fluid).

The assumption of a linear relaxation towards the equilibrium distribution is certainly justified for typical subsonic flow problems in which the macroscopic flow velocity is small compared to the thermal velocities of the particles as depicted in Fig. 3. In these situations, the SRT collision operator can be seen of a first order Taylor expansion of the actual collision operator.

Given the SRT collision operator, the Boltzmann transport equation reads

$$\partial_t f + \boldsymbol{v} \cdot \nabla_x f + \frac{\boldsymbol{F}}{m} \cdot \nabla_v f = \frac{1}{\tau}(f^{\mathrm{eq}} - f). \tag{9}$$

To obtain the desired macroscopic quantities, such as the fluid density $\rho(\boldsymbol{x},t)$, and the flow velocity $\boldsymbol{u}(\boldsymbol{x},t)$, we have to integrate out the unnecessary microscopic degrees of freedom (the molecular velocities). One does so by forming so-called hydrodynamic modes (products of f with powers of $\boldsymbol{v}$). Applying this procedure to the Boltzmann transport equation as a whole, yields information about the following macroscopic quantities:

0^{th} mode: $\int_{\mathbb{R}^3} \cdot f\boldsymbol{v}^0 \,\mathrm{d}^3v$ — Conservation of the particle number (continuity equation),

1^{st} mode: $\int_{\mathbb{R}^3} \cdot f\boldsymbol{v}^1 \,\mathrm{d}^3v$ — Conservation of momentum (Navier-Stokes equations),

2^{nd} mode: $\int_{\mathbb{R}^3} \cdot f(\boldsymbol{v}-\boldsymbol{u})^2 \,\mathrm{d}^3v$ — Conservation of energy (Heat flux equation).

We will explicitly carry out this calculation for the 0^{th} mode and leave the higher modes to the inclined reader [1].

$$\partial_t \overbrace{\int_{\mathbb{R}^3} f \,\mathrm{d}^3v}^{=n} + \partial_\alpha^x \overbrace{\int_{\mathbb{R}^3} v_\alpha f \,\mathrm{d}^3v}^{=nu_\alpha} + \frac{F_\alpha}{m} \overbrace{\int_{\mathbb{R}^3} \partial_\alpha^v f \,\mathrm{d}^3v}^{=0} = \frac{1}{\tau} \overbrace{\int_{\mathbb{R}^3} f^0 - f \,\mathrm{d}^3v}^{=0},$$

where Einstein notation in the index α has been used. Using the normalisation of the distribution function for the first term, the definition of the macroscopic velocity $\boldsymbol{u}$ for the second term, the fact that $f \to 0$ for $|v| \to \infty$ for the third term, as well as the fact that the equilibrium distribution f^{eq} is chosen such that it locally represents the same particle density as the non-equilibrium distribution f for the fourth term. Finally, we end up with

$$\partial_t n + \partial_\alpha(nu_\alpha) = 0, \tag{10}$$

which in vector notation reads

$$\dot{n} + \nabla \cdot (n\boldsymbol{u}) = 0. \tag{11}$$

As expected, this matches the continuity equation (1) apart from units.

The result for the 2^{nd} does not only yield the Navier-Stokes equations, but also the relation between the relaxation time τ in the SRT collision operator and the shear viscosity η of the fluid.

[1] As opposed to the 0^{th} mode, non-trivial expansions and truncations have to be carried out for the higher modes.

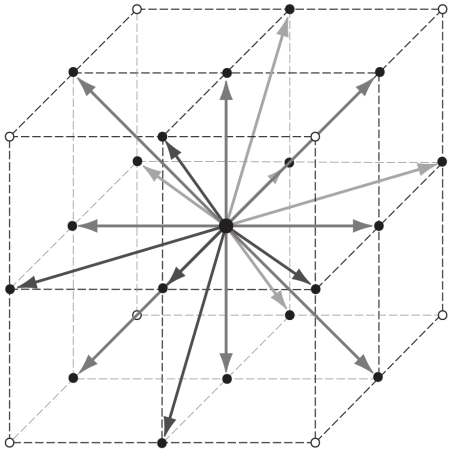

Figure 4. D3Q19 lattice with discrete velocities connecting every node with itself, its nearest, and next nearest neighbors.

V. LATTICE-BOLTZMANN

Lattice-Boltzmann uses a simple finite-difference discretization for the time derivative in the Boltzmann transport equation (7)

$$\frac{d}{dt} f\big(\boldsymbol{x}(t), \boldsymbol{v}(t), t\big) \approx \frac{f\big(\boldsymbol{x}(t) + v(t)\Delta t, \boldsymbol{v}(t), t + \Delta t\big) - f\big(\boldsymbol{x}(t), \boldsymbol{v}(t), t\big)}{\Delta t} \tag{12}$$

Using a regular grid for the spatial coordinate $\boldsymbol{x}$, and a finite number of discrete velocities $\boldsymbol{c}_i$ chosen such that they transport density populations from one grid node to the next in one time step, yields the following explicit propagation scheme:

$$\underbrace{f\big(\boldsymbol{x} + \boldsymbol{c}_i, \boldsymbol{c}_i, t + \Delta t\big) = f\big(\boldsymbol{x}, \boldsymbol{c}_i, t\big)}_{\text{streaming}} + \underbrace{\frac{\Delta t}{\tau}\Big(f^{\text{eq}} - f\big(\boldsymbol{x}, \boldsymbol{c}_i, t\big)\Big)}_{\text{collision}}. \tag{13}$$

A typical choice for such a grid is the D3Q19 grid (3 dimensions, 19 discrete velocities) depicted in Fig. 4.

The discrete scheme is naturally devided into two parts that can be continuously iterated: the streaming step (Fig. 5), during which velocity populations are moved to neighboring nodes according to their lattice velocity; and the collision step (Fig. 6), during which the velocity populations of one grid node are relaxed towards their local equilibrium distribution.

A. Boundary Conditions

Imposing boundary conditions in a lattice-Boltzmann solver is significantly more complicated than in other CFD methods. The reason for this is that macroscopic boundary conditions usually don't contain enough information to reconstruct the a complete set of velocity populations.

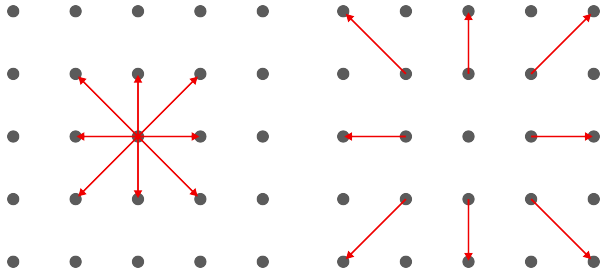

Figure 5. Streaming step on a D2Q8 lattice. The velocity populations are represented as arrows with their respective grid velocities.

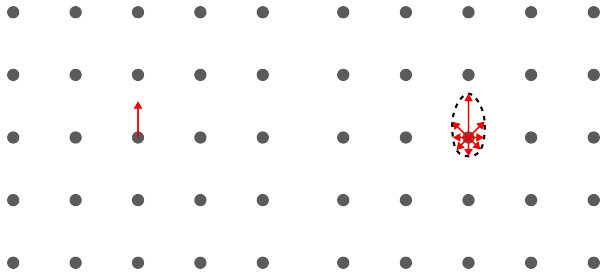

Figure 6. Collision step on a D2Q8 lattice. The velocity populations are represented as arrows with their respective grid velocities.

By today, quite some research has gone into schemes to impose velocity, pressure, and stress boundary conditions. Here we want to discuss only one specific method to impose no-slip boundary conditions — the so-called bounce-back scheme.

Suppose our simulation contains a flat, grid-aligned boundary located right in the middle between two grid nodes. We can then produce no-slip ($\boldsymbol{u} = 0$) boundary conditions through a symmetry argument. Consider a single fluid node at the boundary and its velocity populations as depicted in Fig. 7. Suppose there is a flow on the other side of the boundary going the other way, such that the combined system of real and imagined flow is point symmetric with respect to the position on the boundary at the node under consideration. On this symmetry point, the velocity has to vanish. Due to the point symmetry, for any population entering the wall, there will be an equally large population exiting the wall in the opposite direction. We can therefore simulate no-slip walls by simply bouncing back populations.

This scheme is only exactly correct for grid-aligned walls in between nodes and flow with translational symmetry along the wall. The scheme can be employed for completely asymmetric walls, where it's accuracy is $\mathcal{O}(\Delta x)$.

B. Particle Coupling

The aforementioned bounce-back boundary conditions can be used to represent resting particles — and with

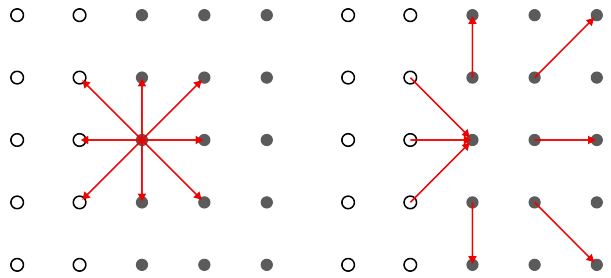

Figure 7. Bounce-back streaming step on a D2Q8 lattice. The filled circles represent fluid nodes, while the empty circles represent boundary nodes.

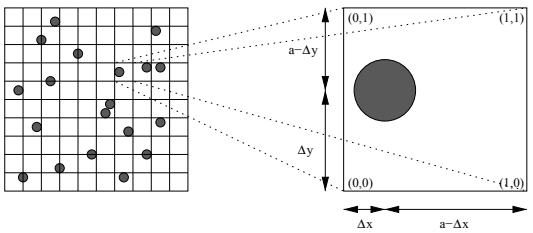

Figure 8. A simple trilinear (bilinear in 2d) scheme can be used to interpolate the fluid flow velocity onto the particle position, and to interpolate the coupling force back into neighboring fluid nodes.

modifications — to also represent moving particles. However, in typical soft matter simulations, it is most often easier and computationally cheaper to represent particles by one or more coupling points that exchange a frictional coupling force between a particle and the fluid. In our case, this coupling force takes the shape of a simple frictional force proportional to the relative velocity of the particle and the local fluid:

$$F = -\gamma(\boldsymbol{v} - \boldsymbol{u}). \tag{14}$$

The main problem here is that the fluid velocity $\boldsymbol{u}$ is only defined on a grid, while the particle positions are unrestricted. This problem can be solved by simply interpolating the fluid velocity from neighboring nodes onto the particle position using a trilinear scheme as shown in Fig. 8, calculating the coupling force using Eq. (14), and interpolating the equal and opposite force back onto the fluid nodes using the same interpolation scheme.

This coupling scheme results in a mobility of the particle with several contributions stemming from the relative motion of the particle and the local fluid, the motion of the fluid, and periodic boundary conditions (if present) as shown in Fig. 9. Expressions for the individual contributions can be found in Dünweg and Ladd [1].

VI. THERMALIZATION

In a simulations of an NVT ensemble, there need to be fluctuations compensating the energy loss of any dissipative interaction (generally frictional interactions) causes.

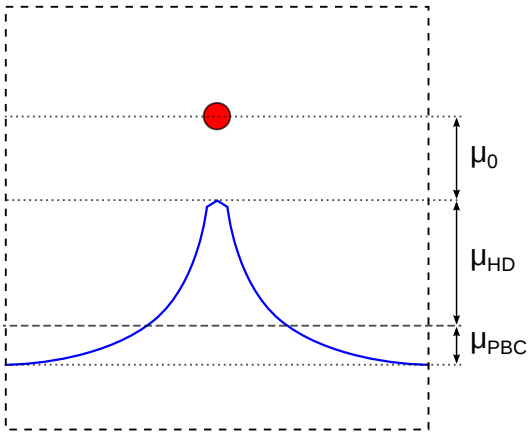

Figure 9. Different contributions to the mobility of a particle with point coupling to a lattice-Boltzmann fluid. The mobility is determined by a combination of the friction parameter in the coupling force, the hydrodynamic momentum transport, the periodic boundary conditions, as well as a small contribution from the grid interpolation scheme.

If these fluctuations are not properly introduced into the simulation, then the temperature will be incorrect, which leads to, e.g. massively incorrect polymer conformations.

The only dissipative interactions in the LB algorithm as presented so far, are the particle coupling force and the viscous friction in the LB fluid. The particle coupling can be thermalized using a Langevin type scheme: in addition to the frictional force, there need to be uncorrelated random forces $\boldsymbol{R}(t)$ acting between the particles and the fluid, with a variance given by the fluctuation-dissipation relation

$$\langle \boldsymbol{R}(t) \cdot \boldsymbol{R}(t') \rangle = 2\gamma k_B T \, \delta(t - t'). \tag{15}$$

The situation is more complicated for the fluid. The fluctuations need not break mass and momentum conservation. We can therefore not apply random forces. The correct quantity to apply fluctuations to is the stress tensor, randomizing the momentum flux. Going back to the general form of the conservation of momentum Eq. (2), we can express this as

$$\nabla \cdot \left(\bar{\boldsymbol{\Pi}} + \bar{\boldsymbol{\Pi}}_{\mathrm{R}} \right) = -\partial_t(\rho \boldsymbol{u}) + \boldsymbol{f}, \tag{16}$$

with the symmetric random tensor $\bar{\boldsymbol{\Pi}}_{\mathrm{R}}$. Since the dissipative interaction associated with these fluctuations is viscous friction, we expect there to be a fluctuation-dissipation relation for the individual components of $\bar{\boldsymbol{\Pi}}_{\mathrm{R}}$ similar to Eq. (15), but proportional to the viscosity η instead of γ. Such relations indeed exist and are given in Refs.[1,2].

A more interesting problem is how to actually implement this in the LB scheme. An elegant method to make the stress tensor directly accessible duing the simulation is the so-called multi relaxation time (MRT) collision operator. This collision operator generalized the single relaxation time collision operator by making use of the

fact that there is no physical reason demanding that all populations relax at the same rate. Instead it uses a general linear relaxation as denoted by the relaxation matrix $\bar{\boldsymbol{L}}$

$$\underbrace{f_i(\boldsymbol{x}+\boldsymbol{c}_i, t+\Delta t) = f_i(\boldsymbol{x}, t)}_{\text{streaming}} + \underbrace{L_{ik}\left(f_k^{\text{eq}} - f_k(\boldsymbol{x}, t)\right)}_{\text{collision}}. \tag{17}$$

One constructs $\bar{\boldsymbol{L}}$ switching the basis for the representation of the populations to so-called modes m_i, which represent physical quantities:

$$m_0 = \rho \propto \sum_i f_i, \tag{18}$$

$$m_{1-3} = \boldsymbol{u} \propto \sum_i f_i \boldsymbol{c}_i, \tag{19}$$

$$m_{4-9} = \bar{\boldsymbol{\Pi}} \propto \sum_i f_i\, \boldsymbol{c}_i \otimes \boldsymbol{c}_i. \tag{20}$$

The modes m_{10-18} in the D3Q19 scheme do not directly correspond to any macroscopic quantities and are referred to as kinetic or ghost modes.

The relaxation matrix $\bar{\boldsymbol{L}}$ becomes diagonal in this basis and contains the relaxation factors for the individual modes on its diagonal. The relaxation factor for the modes m_{0-3}, $\gamma_{0-3} = 0$, which enforces mass and momentum conservation. In an isotropic fluid, there are two independent relaxation rates γ_{s} and γ_{b} for the shear and bulk stress modes m_{4-9}. These are related to the shear and bulk viscosity and the relations are given in Refs.[1,2].

Since the stress tensor is now explicitly accessible through the modes m_{4-9}, we can just add the required fluctuations during the collision step.

The expression for the stress tensor $\bar{\boldsymbol{\Pi}}$ Eq. (20) can be understood by considering that $\boldsymbol{c}_i \otimes \boldsymbol{c}_i$ projects a given vector onto the direction of the velocity of the population f_i. This is because the LB model is based on non-interacting particles, who transport momentum of the direction if their motion, in the direction of their motion. The momentum flux $\bar{\boldsymbol{\Pi}}$ needs to scale quadratically with $\boldsymbol{c}_i$, since both the amount of momentum carried, and the speed at which it is transported, is given by the velocity $\boldsymbol{c}_i$.

VII. FURTHER READING

For more detailed derivations and further information, we recommend Dünweg and Ladd [1], as well as Schiller [2], and Wagner [3].

REFERENCES

[1] B. Dünweg and A. J. C. Ladd (Springer Berlin Heidelberg, 2008) pp. 1–78.

[2] U. D. Schiller, "Thermal fluctuations and boundary conditions in the lattice boltzmann method,".

[3] A. J. Wagner (Department of Physics, North Dakota State University, 2008).